

Miniaturization of Normal-State and Superconducting Striplines†

R. L. Kautz*

Center for Electronics and Electrical Engineering, National Bureau of Standards, Boulder, Colorado 80303

December 19, 1978

The properties of normal-state and superconducting striplines are calculated as a function of miniaturization. For normal conductors the Reuter-Sondheimer theory is applied in order to account for the effects of finite film thickness and mean free path. For superconductors the Mattis-Bardeen theory is used in order to include effects due to the energy gap. Calculations for three example conductors, copper at 295 K and 4.2 K and niobium at 4.2 K, examine the attenuation, dispersion, and characteristic impedance of striplines as a function of frequency and dielectric thickness. Simulations of pulse transmission are used to evaluate the utility of the example striplines for high-speed digital applications.

Key words: Copper; niobium; stripline; superconductivity; surface impedance.

I. Introduction

Striplines interconnect the active devices of both semiconductor and Josephson-junction high-speed integrated circuits. The desirability of high device densities, particularly for digital circuits, provides motivation for the miniaturization of all circuit components, including striplines. At present, device densities for semiconductor logic circuits having 100 ps propagation delays are limited to about 25 gates per chip, simply because each gate consumes 40 mW of power [1]¹. In contrast, Josephson-junction circuits of comparable speed require only about one thousandth as much power [2] and correspondingly higher device densities are anticipated [3]. While power dissipation presently limits the scale of integration for high-speed semiconductor circuits, it has also been noted that the normal-metal interconnections used in such circuits degrade much more rapidly with miniaturization than the superconducting interconnections of Josephson-junction circuits [4]. Here we present detailed calculations comparing the properties of normal-state and superconducting striplines.

The stripline geometry to be considered is shown in figure 1. For striplines typical of semiconductor circuits, the conductor and dielectric thickness, d and s , are 1 and 200 μm respectively [5], while for superconducting circuits these dimensions are both around 0.2 μm [6]. Thus, although the conductors are of roughly the same thickness in both technologies, the dielectric thicknesses differ by three orders of

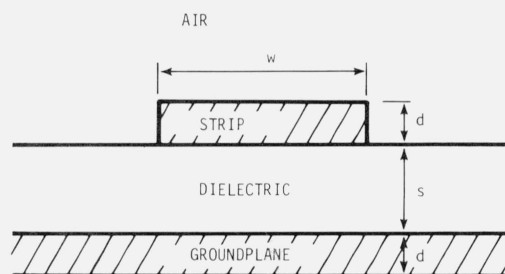


FIGURE 1. Stripline geometry in cross-section.

magnitude. The thinner dielectric of the superconducting circuit permits higher device densities for two reasons. First, because the characteristic impedance of a stripline is, to a good approximation, a function only of the dielectric constant and the ratio of strip width to dielectric thickness w/s , shrinking the dielectric layer permits smaller strip widths while maintaining the same impedance level. Second, because adjacent striplines become coupled if the separation between them is less than a few dielectric thicknesses [7], thinning the dielectric layer permits closer spacing of the striplines while avoiding crosstalk. The actual strip widths used in semiconducting and superconducting circuits are typically 100 μm [5] and 5 μm [8] respectively, and differ by less than a factor of 10^3 primarily because different impedance levels are appropriate for the active devices of the two technologies. For present superconducting circuits, crosstalk can probably be avoided if striplines are separated by 1 μm , while for semiconducting circuits a separation of at least 400 μm is required. One concludes that the miniaturization

† Partially supported by the Office of Naval Research under contract number N00014-77-F-0048, dated May 1, 1977.

* NRC-NBS Postdoctoral Research Associate, Electromagnetic Technology Division.

¹ Figures in brackets indicate literature references at the end of this paper.

zation of striplines beyond their present size in semiconductor circuits can proceed without reduction of the conductor thickness but not without thinning the dielectric.

As will be shown, both radiation and dielectric losses become relatively less important compared to conductor losses as the dielectric thickness is reduced. For the purpose of this study, it thus proves sufficient to focus on the effects associated with imperfect conductors, assuming a lossless dielectric and neglecting radiation. The effect of miniaturization is considered for striplines made from three different conductors, copper at 295 K and 4.2 K and niobium at 4.2 K. These conductors represent respectively, a normal metal exhibiting the normal and anomalous skin effects (at the frequencies of interest) and a superconductor.

To further simplify the calculations, we consider only the TEM mode and the stripline width is taken to be much greater than the dielectric thickness, $w \gg s$, such that fringing fields can be neglected. These assumptions eliminate dispersion associated with the discontinuity in dielectric constant at the air/dielectric interface, an important source of dispersion for w comparable to or smaller than s [9, 10]. One notes, however, that for the TEM mode such dispersion can be reduced to an arbitrary magnitude by overlaying the stripline with a dielectric layer of sufficient thickness.

Under the above assumptions the properties of a stripline follow almost immediately once the surface impedance of the conductor is calculated. In section 2, expressions for the surface impedance of both normal-metals and superconductors of finite thickness are reviewed. These expressions are used in section 3 to evaluate the attenuation, phase velocity, and characteristic impedance as a function of dielectric thickness assuming a fixed conductor thickness of 1 μm . Section 4 looks at the propagation of short pulses over various lengths of stripline.

2. Surface Impedance

The surface impedance required here is a quantity which abstracts information about the penetration of fields into an infinite conducting slab of thickness d . Taking the surfaces of the conductor as the planes $z = 0$ and $z = d$, the surface impedance is defined for a sinusoidal electric field $E_x(z, \omega)e^{i\omega t}$ and current density $J_x(z, \omega)e^{i\omega t}$ by

$$Z_s(\omega) = \frac{E_x(0, \omega)}{\int_0^d dz J_x(z, \omega)}, \quad (2.1)$$

with the boundary condition that the magnetic field be zero at $z = d$ as is appropriate for a stripline with $w \gg s$. The real part of Z_s , called the surface resistance, accounts for stripline losses and the imaginary part, the surface reactance, contributes to the stripline inductance.

Evaluation of the surface impedance for copper at 295 K and niobium at 4.2 K is simplified by the fact that \mathbf{J} and \mathbf{E} are related by the local equation

$$\mathbf{J} = \sigma \mathbf{E}, \quad (2.2)$$

where σ is the complex conductivity. This local equation can be assumed because the mean free path l for normal electrons is short compared to all other dimensions in the problem. Combining eq. (2.2) with Maxwell's equations yields for the surface impedance [11]

$$Z_s = (i\omega\mu_o/\sigma)^{1/2} \coth [(i\omega\mu_o\sigma)^{1/2}d] \quad (2.3)$$

The surface impedance thus follows once the conductivity is known. For copper σ is simply a real constant. For superconducting niobium, σ is a complex, frequency-dependent quantity which we take to be of the form given by Mattis and Bardeen [12]. The Mattis-Bardeen equation yields the conductivity of a superconductor at a given frequency and temperature provided two material parameters are known; the energy gap parameter Δ and the normal state conductivity at the superconducting transition temperature σ_n . A more complete account of the application of Mattis-Bardeen theory to superconducting striplines has been given elsewhere [13].

In the derivation of eq. (2.3) for the case of infinite conductor thickness, it is observed that the field amplitudes decay exponentially with distance into the conductor. For a normal metal the characteristic decay length is the classical skin depth

$$\delta_c = (\omega\mu_o\sigma/2)^{-1/2}. \quad (2.4)$$

Because δ_c decreases with increasing frequency there exists a frequency above which $\delta_c < l$ and a local relation between \mathbf{J} and \mathbf{E} can no longer be assumed. At such high frequencies the skin effect is said to be anomalous. For a superconductor, the decay length at frequencies less than the energy gap frequency, $2\Delta/\hbar$, is the penetration depth [14]

$$\lambda = (\hbar \coth(\Delta/2kT)/\pi\mu_o\Delta\sigma_n)^{1/2}, \quad (2.5)$$

which, in contrast to δ_c , is frequency independent. In the process of miniaturizing striplines, the depth of field penetration plays an increasingly important role as the dielectric thickness is reduced.

Because the mean free path of copper at 4.2 K can be long compared to both δ_c , and d , the relation between \mathbf{J} and \mathbf{E} assumes the non-local form [15]

$$\mathbf{J}(\mathbf{r}) = \frac{3\sigma}{4\pi l} \int d^3\rho \boldsymbol{\rho} (\boldsymbol{\rho} \cdot \mathbf{E}(\mathbf{r} + \boldsymbol{\rho})) \rho^{-4} e^{-\rho/l}, \quad (2.6)$$

where we have assumed that the relaxation time τ is small compared to the inverse frequency, $\omega\tau \ll 1$. Evaluation of

the surface impedance in this case requires an additional boundary condition regarding the scattering of electrons from the conductor surface. Of the two simple limits, diffuse scattering and specular reflection, the former seems to provide the better agreement with experiment [15] and has been assumed in the present calculations. Equation (2.4) and Maxwell's equations applied to the surface problem with diffuse scattering yield [15].

$$\frac{d^2 E_x}{dz^2} = i\alpha l^{-3} \int_0^d dz' E_x(z') K((z' - z)/l) \quad (2.7)$$

$$K(u) = \int_1^\infty dr \left[\frac{1}{r} - \frac{1}{r^3} \right] e^{-|u|/r}$$

where $\alpha = 3/2 l^2 / \delta_c^2$. Reuter and Sondheimer [16] solved this equation in the limit of infinite d and obtain for the surface impedance

$$Z_s = i \frac{4\pi}{3} \frac{\alpha}{\sigma l} \left[\int_0^\infty dt \ln(1 + i\alpha k(t)/t^2) \right]^{-1} \quad (2.8)$$

$$k(t) = \frac{2}{t^3} [(1 + t^2) \tan^{-1}(t) - t].$$

For $\alpha \ll 1$, (normal skin effect), this expression reduces to the $d = \infty$ limit of eq (2.3). For $\alpha \gg 1$ (extreme anomalous skin effect), Reuter and Sondheimer obtain

$$Z_s = \frac{1}{3^{1/2} \pi^{1/3}} (1 + \sqrt{3} i) \frac{\alpha^{2/3}}{\sigma l}, \quad \alpha \gg 1, \quad (2.9)$$

The expressions for the surface impedance of a normal metal given above are valid either for $l \ll \delta_c$, d (eq (2.3)) or for arbitrary l and $d = \infty$ (eq (2.8)). The numerical solution of eq (2.7) and calculation of the surface impedance for arbitrary l , δ_c , and d is discussed in the appendix. The resulting general program was used to obtain all results for normal metals presented here.

Although the fields do not fall off in a precisely exponential way for the anomalous skin effect, it remains possible to define a characteristic penetration length. In general, the distance over which the field amplitude decays is given by

$$\delta = \frac{1}{\omega \mu_o \operatorname{Re}[Z_s]} |Z_s|^2 \quad (2.10)$$

In the local limit this reduces to δ_c for a normal metal and to λ for a superconductor. In the extreme anomalous limit, eq (2.9) may be used to obtain

$$\delta_a = \frac{2^{1/3} 3^{1/6}}{\pi^{1/3}} (\delta_c^2 l)^{1/3}. \quad (2.11)$$

so that the skin depth for $l > \delta_c$ is greater than δ_c .

TABLE I. Material Parameters.

	$\sigma(\Omega^{-1}m^{-1})$	$l(m)$	$\tau(s)$	
Cu, 295 K	5.88×10^7	3.82×10^{-8}	2.34×10^{-14}	
Cu, 4.2 K	2.94×10^{10}	1.91×10^{-5}	1.19×10^{-11}	
	$\sigma_n(\Omega^{-1}m^{-1})$	$l(m)$	$\Delta(meV)$	$\lambda(m)$
Nb, 4.2 K	1.57×10^7	1.1×10^{-8}	1.48	8.6×10^{-8}

The material parameters of copper and niobium used here are presented in table 1. The conductivity of copper at room temperature [17] is limited by phonon scattering and all specimens have nearly the same value. At 4.2 K scattering from impurities and defects dominate and, although the conductivity can be more than 10^4 times that at 295 K for specially prepared samples, a residual resistance ratio of 10^2 is common for off-the-shelf wires [18]. Here we assume, perhaps optimistically, that the conductivity at 4.2 K is 500 times the room temperature value. The mean free path is derived from the fact that σ/l is approximately constant for a given material and has a value of $1.54 \times 10^{15} \Omega^{-1} m^{-2}$ for copper [11]. The relaxation time is calculated from

$$\tau = l/v_F, \quad (2.12)$$

where the Fermi velocity v_F is 1.6×10^6 m/s for copper [11]. Material parameters for superconducting niobium are based on the thin-film measurements of Henkels and Kircher [19].

The measured value of σ_n , $1.59 \times 10^7 \Omega^{-1} m^{-1}$, was modified slightly so that eq (2.5) is exactly satisfied.

The real and imaginary parts of the surface impedance of the three example metals are shown in figure 2 for a metal thickness of $1 \mu m$. Because the mean free path is much shorter than the film thickness, the surface impedance of copper at 295 K is described by the local formula, eq. (2.3), for frequencies below about 3×10^{12} Hz. Above this frequency, the classical skin depth is smaller than the mean free path and the skin effect is anomalous. At sufficiently low frequencies δ_c is large compared to the conductor thickness and eq (2.3) reduces to

$$Z_s = \frac{1}{\sigma d} + i \frac{1}{3} \omega \mu_o d, \quad l \ll d \ll \delta_c. \quad (2.13)$$

This equation, which results when the electric field is uniform across the conductor thickness, accounts for the impedance of copper at 295 K and below about 4×10^9 Hz

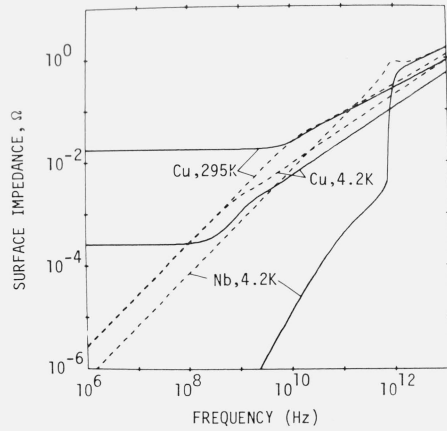


FIGURE 2. The real (solid line) and imaginary (dashed line) parts of the surface impedance for $1\ \mu\text{m}$ thick films of copper at 295 K and 4.2 K and niobium at 4.2 K.

The results for copper at 4.2 K and frequencies above 10^{12} Hz may be inaccurate due to the omission of relaxation-time effects.

shown in figure 2. At higher frequencies δ_c becomes small compared to d and eq 2.3 reduces to

$$Z_s = (1 + i) \left(\frac{\omega \mu_o}{2\sigma} \right)^{1/2}, \quad l \ll \delta_c \ll d. \quad (2.14)$$

In this limit the electric field decays exponentially to a small value before reaching the back surface of the conductor.

At 4.2 K the mean free path of copper is sufficiently long that δ_c is comparable to l even at 2×10^4 Hz. Thus, the anomalous skin effect is exhibited over the entire frequency range of figure 2. The relaxation time is sufficiently long at 4.2 K that $\omega\tau$ is unity at 10^{10} Hz (compared to 7×10^{12} Hz at room temperature). Pippard [15] has shown, however, that in the extreme anomalous limit, relaxation-time effects are important only when $\omega\tau$ is considerably greater than unity and in the present case need not be considered for frequencies less than about 10^{12} Hz. Since the relaxation time has been neglected, the results shown in figure 2 for copper at 4.2 K are probably not accurate above this frequency. As at room temperature, the surface impedance at 4.2 K depends critically on whether the skin depth is greater or less than the conductor thickness. The break point occurs when $\delta_a = d$ or about 2×10^8 Hz. Below this frequency, Z_s is given by an equation similar to eq (2.13) in which the bulk conductivity σ is replaced by an apparent conductivity $\bar{\sigma}$ that accounts for the effect of finite conductor thickness on the mean free path [20]. In the present case, the apparent conductivity is 0.13 times the bulk conductivity. At frequencies above 2×10^8 Hz we have $\delta_c \ll l, d$ and eq (2.9) applies. As can be easily verified from eq (2.9), the surface impedance in this region depends only on σ/l , a constant of the material, and

thus does not depend on the somewhat arbitrarily chosen residual resistivity ratio. If, for example, the resistivity ratio had been taken as 5000 rather than 500, the only significant change in the surface impedance would be a six-fold decrease in $Re[z_s]$ below 2×10^8 Hz. These considerations have been discussed in detail by Keyes et al. [4].

Below the energy gap frequency, 7.2×10^{11} Hz for Nb at 4.2 K, the surface resistance of a superconductor is orders of magnitude smaller than that of a normal metal. In a stripline the smaller surface resistance results in lower attenuation. Also, the surface reactance below the energy gap varies as ω , making it appear exactly as an inductance. This property yields a stripline with very low dispersion. Above the energy gap, a superconductor behaves like a normal metal of conductivity σ_n .

3. Propagation Constant and Characteristic Impedance

The propagation constant γ and characteristic impedance Z_o of a stripline can be expressed in terms of the series impedance Z and shunt admittance Y of a unit length of line,

$$\gamma = \sqrt{ZY}. \quad (3.1)$$

$$Z_o = \sqrt{Z/Y}. \quad (3.2)$$

where Z and Y for $w \gg s$ are in turn [11]

$$Z = i\omega\mu_o \frac{s}{w} + \frac{2}{w} Z_s, \quad (3.3)$$

$$Y = i\omega\epsilon\epsilon_o \frac{w}{s}, \quad (3.4)$$

The first term of Z is the inductive impedance associated with the magnetic field in the dielectric region and the second term accounts for penetration of fields into the conductor. Y is the capacitive admittance between the strip and the ground plane. In the following calculations a relative dielectric constant ϵ of 4 is arbitrarily assumed. Note that γ is independent of w while Z_o is proportional to $1/w$. Thus, both γ and $\frac{w}{s} Z_o$ can be calculated without specifying the stripline width. The power attenuation in decibels per length α_{dB} and the phase velocity v_ϕ are related to the real and imaginary parts of γ by

$$\alpha_{dB} = C_{dB} Re[\gamma], \quad (3.5)$$

$$v_\phi = \omega/Im[\gamma], \quad (3.6)$$

where $C_{dB} = 20 \log_{10} e$. The properties of a stripline thus follow from the surface impedance of the conductor.

The phase velocity, attenuation, and characteristic impedance of a room temperature copper stripline are shown in figure 3 for a conductor thickness of $1 \mu\text{m}$ and a dielectric thickness ranging from $200 \mu\text{m}$ to $0.2 \mu\text{m}$. As the dielectric thickness is reduced toward $0.2 \mu\text{m}$, the line becomes highly dispersive and lossy and develops a characteristic impedance far from the real, frequency-independent impedance of an ideal line. As a function of frequency the degradation of a fixed length of line due to loss and dispersion increases with increasing frequency. This increase in dispersion is less than obvious since the phase velocity approaches a constant at high frequencies but will be explained presently. Problems with impedance matching are reduced at high frequencies as the characteristic impedance approaches a real constant.

A better understanding of the results shown in figure 3 can be obtained by reviewing approximate expressions for γ and Z_o applicable in the four regions bounded by dotted lines. These regions are defined by

$$\text{I. } d, \sqrt{sd} \ll \delta_c$$

$$\text{II. } d \ll \delta_c \ll \sqrt{sd}$$

$$\text{III. } \delta_c \ll s, d$$

$$\text{IV. } s \ll \delta_c \ll d$$

and result from the two possible forms for the surface impedance, eqs (2.13) and (2.14), combined with two possibilities for the series impedance of eq (3.3), either resistive or reactive. Of the four regions, I, II, and III are of principal interest here since condition IV is satisfied only for the $0.2 \mu\text{m}$ dielectric case over a narrow range of frequencies.

The asymptotic forms for the phase velocity in the regions of interest are

$$\text{I. } v_\phi = \sqrt{\frac{\omega s d \sigma}{\epsilon \epsilon_0}} \left[1 - \frac{1}{3} \frac{d^2}{\delta_c^2} - \frac{1}{2} \frac{s d}{\delta_c^2} \right], \quad (3.7)$$

$$\text{II. } v_\phi = \frac{1}{\sqrt{\mu_0 \epsilon \epsilon_0}} \left[1 - \frac{1}{3} \frac{d}{s} - \frac{1}{8} \frac{\delta_c^4}{s^2 d^2} \right] \quad (3.8)$$

$$\text{III. } v_\phi = \frac{1}{\sqrt{\mu_0 \epsilon \epsilon_0}} \left[1 - \frac{1}{2} \frac{\delta_c}{s} \right] \quad (3.9)$$

where correction terms have been indicated in brackets. As figure 3 indicates, approximations I, II, and III become valid at successively higher frequencies. In the lowest frequency range v_ϕ is proportional to $\sqrt{\omega}$ and goes to zero at zero frequency. If, however, one considers the phase shift that results because the low frequencies travel at a velocity less than the high-frequency asymptotic velocity then for a fixed length of line ℓ this phase shift

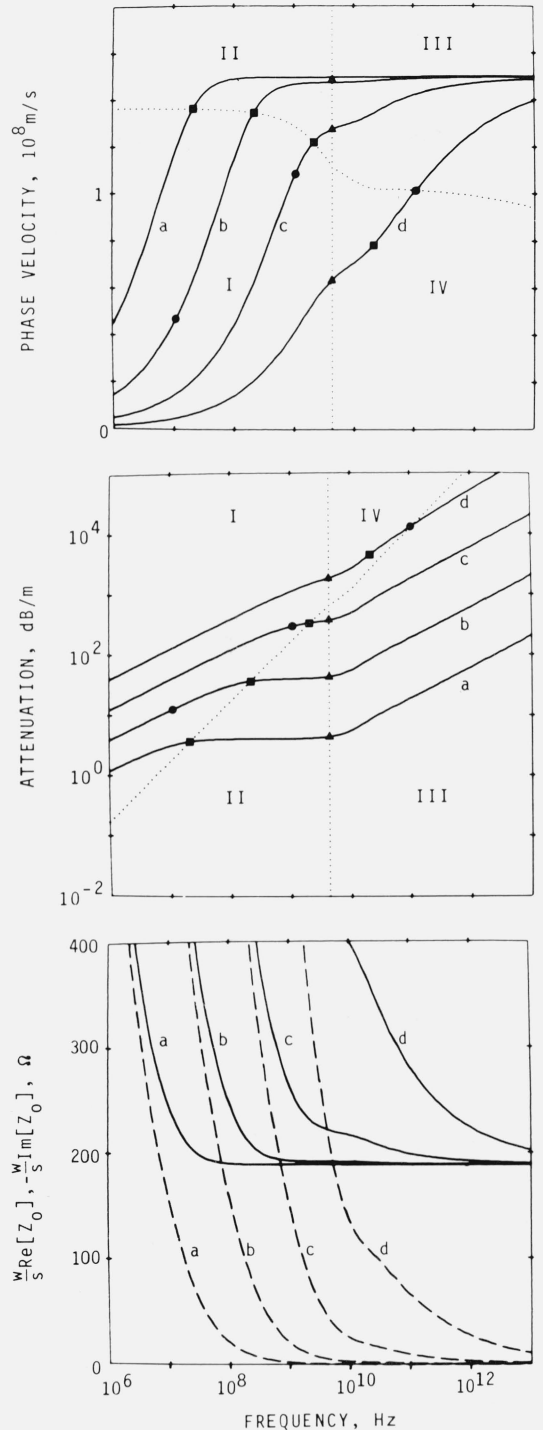


FIGURE 3. Phase velocity, attenuation, and real (solid line) and imaginary (dashed line) parts of the characteristic impedance of a 295 K copper stripline with $1 \mu\text{m}$ conductor thickness.

Results are shown for a relative dielectric constant of 4 and dielectric thicknesses of $200 \mu\text{m}$ (a), $20 \mu\text{m}$, (b) $2 \mu\text{m}$, (c), and $0.2 \mu\text{m}$ (d). Dotted lines divide the graphs of phase velocity and attenuation into regions where simple approximate equations hold. Circles, squares, and triangles mark points at which $\delta_c = s$, $\delta_c = \sqrt{sd}$, and $\delta_c = d$, respectively.

$$\Delta\phi = \omega\ell \left(\frac{1}{v_\phi(\omega)} - \frac{1}{v_\phi(\infty)} \right),$$

also goes to zero at zero frequency as $\sqrt{\omega}$. Thus, dispersion at low frequencies is not the problem that figure 3 suggests. At somewhat higher frequencies δ_c becomes less than \sqrt{sd} and approximation II applies. In this region v_ϕ approaches the asymptotic value $(1 - d/3s)/\sqrt{\mu_o\epsilon\epsilon_o}$ with a correction term which decreases as ω^{-2} with increasing frequency. Finally, as δ_c becomes less than d as well as s , v_ϕ approaches $1/\sqrt{\mu_o\epsilon\epsilon_o}$ with a correction term of $-\delta_c/2s$. Because this term goes as $1/\sqrt{\omega}$, the phase shift $\Delta\phi$ goes as $\sqrt{\omega}$ and dispersion effects increase with ω just as at very low frequencies. Also note that the correction term is proportional to $1/s$ so that thin dielectrics enhance dispersion.

The attenuation can be approximated in the regions of interest by

$$\text{I. } \alpha_{dB} = C_{dB} \sqrt{\frac{\omega\epsilon\epsilon_o}{sd\sigma}} \cdot \left[1 - \frac{1}{3} \frac{d^2}{\delta_c^2} - \frac{1}{2} \frac{sd}{\delta_c^2} \right], \quad (3.10)$$

$$\text{II. } \alpha_{dB} = \frac{C_{dB}}{\sigma sd} \sqrt{\frac{\epsilon\epsilon_o}{\mu_o}} \left[1 - \frac{1}{3} \frac{d}{s} + \frac{4}{45} \frac{d^4}{\delta_c^4} \right], \quad (3.11)$$

$$\text{III. } \alpha_{dB} = \frac{C_{dB}}{s} \sqrt{\frac{\omega\epsilon\epsilon_o}{2\sigma}} \left[1 - \frac{1}{2} \frac{\delta_c}{s} \right]. \quad (3.12)$$

As a function of frequency, α_{dB} increases as $\sqrt{\omega}$ at very low and very high frequencies with a frequency independent plateau in between. As a function of dielectric thickness, α_{dB} always increases with decreasing dielectric thickness, either as $1/\sqrt{s}$ or as $1/s$.

Lastly, the characteristic impedance is approximated by

$$\text{I. } Z_o = \frac{1}{w} \sqrt{\frac{s}{\omega\epsilon\epsilon_o\sigma d}} \left\{ \left[1 + \frac{1}{3} \frac{d^2}{\delta_c^2} + \frac{1}{2} \frac{sd}{\delta_c^2} \right] - i \left[1 - \frac{1}{3} \frac{d^2}{\delta_c^2} - \frac{1}{2} \frac{sd}{\delta_c^2} \right] \right\} \quad (3.13)$$

$$\text{II. } Z_o = \frac{s}{w} \sqrt{\frac{\mu_o}{\epsilon\epsilon_o}} \left\{ \left[1 + \frac{1}{3} \frac{d}{s} + \frac{1}{8} \frac{\delta_c^4}{s^2 d^2} \right] - i \frac{1}{2} \frac{\delta_c^2}{sd} \left[1 - \frac{1}{3} \frac{d}{s} + \frac{4}{45} \frac{d^4}{\delta_c^2} \right] \right\}, \quad (3.14)$$

$$\text{III. } Z_o = \frac{s}{w} \sqrt{\frac{\mu_o}{\epsilon\epsilon_o}} \left\{ \left[1 + \frac{1}{2} \frac{\delta_c}{s} \right] - i \frac{1}{2} \frac{\delta_c}{s} \left[1 - \frac{1}{2} \frac{\delta_c}{s} \right] \right\}. \quad (3.15)$$

In the limit of low frequencies the real and imaginary parts of Z_o both diverge as $1/\sqrt{\omega}$. The significance of this divergence relates to the reduction of the transmission line to a simple resistor at low frequencies. For $\delta_c < s, d$ the real part of Z_o approaches its high frequency asymptote, $\frac{s}{w} \sqrt{\mu_o/\epsilon\epsilon_o}$, and the imaginary part goes to zero. The correction term to the real part is $\delta_c/2s$ so that the dielectric thickness directly influences the ability to match impedances over a wide range of frequencies.

The properties of copper and niobium striplines at 4.2 K are shown in figure 4, again for a conductor thickness of 1 μm and dielectric thicknesses ranging from 200 μm to 0.2 μm . Comparing copper at 295 K and 4.2 K shows that the 500 fold increase in conductivity which might result from cooling leads to substantial improvements, especially at low frequencies. These improvements becomes less significant at frequencies approaching 3×10^{12} Hz, where the skin effect becomes anomalous even for copper at 295 K. The superiority of a superconducting stripline at frequencies below $2\Delta/\hbar$ is at once apparent from figure 4. In this region v_ϕ is independent of frequency, α_{dB} is orders of magnitude below the attenuation for a normal conductor, and the characteristic impedance is a real constant. Above 7.2×10^{11} Hz all of these desirable properties disappear as the superconductor begins to behave like a normal conductor.

As for the normal skin effect case at 295 K, simple approximate formulas can be derived for the properties of a stripline in the extreme anomalous limit. The regions of approximation are defined as for the normal skin effect except that δ_c is replaced by δ_a . These regions can be located in figure 4 by using the points marked with circles ($\delta_a = s$), squares ($\delta_a = \sqrt{sd}$), and triangles ($\delta_a = d$) as guides.

At frequencies less than $2\Delta/\hbar$ simple approximations also exist for the parameters of a superconducting stripline [11, 13]. The phase velocity is

$$v_\phi = \frac{1}{\sqrt{\mu_o\epsilon\epsilon_o}} \left(1 + \frac{2\lambda}{s} \coth \frac{d}{\lambda} \right)^{-1/2}, \quad \omega \ll 2\Delta/\hbar. \quad (3.16)$$

While this equation is similar to eq (3.9) for a normal metal, it differs critically in that λ , as opposed to δ_c , is independent of frequency. Thus, as s decreases v_ϕ also decreases but remains frequency independent. The attenuation is

$$\alpha_{dB} = C_{dB} \mu_o^{3/2} \epsilon_o^{1/2} \epsilon_o^{1/2} \frac{\omega^2 \lambda^3 \sigma_1}{2s} \left(1 + \frac{2\lambda}{s} \coth \frac{d}{\lambda} \right)^{-1/2} \times \left(\coth \frac{d}{\lambda} + \frac{d/\lambda}{\sinh^2 d/\lambda} \right), \quad \omega \ll 2\Delta/\hbar. \quad (3.17)$$

where σ_1 is the real part of the conductivity. Because σ_1 is only weakly frequency dependent, α_{dB} is nearly proportional

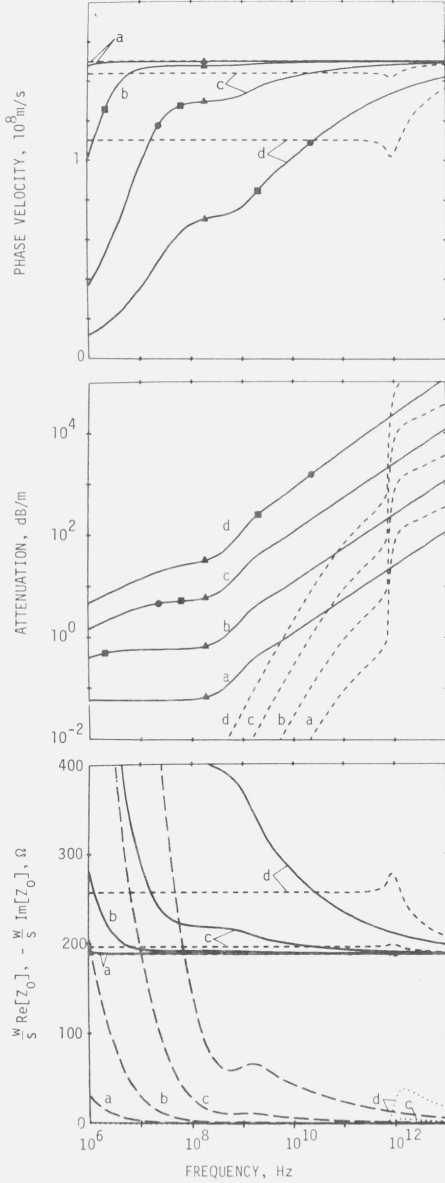


FIGURE 4. Graphs analogous to figure 3 for copper at 4.2 K (solid lines except long dashes for $\text{Im}[Z_0]$) and niobium at 4.2 K (short dashes except dots for $\text{Im}[Z_0]$).

For copper, circles, squares, and triangles mark the points at which $\delta_a = s$, $\delta_a = \sqrt{sd}$, and $\delta_a = d$, respectively.

to ω^2 . For the striplines considered here $\lambda \ll s, d$ and the attenuation is proportional to $1/s$. The characteristic impedance is

$$Z_o = \frac{s}{w} \sqrt{\frac{\mu_o}{\epsilon \epsilon_o}} \left(1 + \frac{2\lambda}{s} \coth \frac{d}{\lambda} \right)^{1/2}, \quad \omega \ll 2\Delta/\hbar, \quad (3.18)$$

which like v_ϕ changes with s but remains frequency independent. The imaginary part of Z_o is negligible. Thus, for $\omega \ll 2\Delta/\hbar$, the only serious deterioration of superconducting stripline properties with miniaturization involves the attenuation.

Before discussing how the transmission of pulses is affected by stripline properties, we briefly examine the two sources of loss, dielectric and radiation, which were neglected in the above calculations. Dielectric losses occur when ϵ has a non-zero imaginary part such that $\epsilon = \epsilon' + i\epsilon''$. Assuming $\epsilon'' \ll \epsilon'$ and a perfect conductor ($Z_s = 0$), the attenuation due to dielectric loss is

$$\alpha_{dB} = \frac{1}{2} C_{dB} \sqrt{\mu_o \epsilon'} \epsilon_o \frac{\epsilon''}{\epsilon'} \omega. \quad (3.19)$$

For many materials ϵ' and ϵ'' are approximately independent of frequency and α_{dB} increases roughly as ω . For good dielectrics ϵ''/ϵ' is typically 10^{-4} at 10^{10} Hz [21] yielding, for $\epsilon' = 4$, an attenuation of 0.2 dB/m. Because this attenuation is independent of s , the conduction losses will always dominate for small enough s . As can be seen from figures 3 and 4, conduction losses at 10^{10} Hz are greater than 0.2 dB/m for all the normal-state lines considered and for the superconducting lines with $s' = 2 \mu\text{m}$ and $0.2 \mu\text{m}$. Because 0.2 dB/m represents a small loss over distances typical of a microcircuit, neglecting dielectric loss will not affect the conclusions of section 4.

A comparison of radiation and conduction losses is complicated by the fact that radiation losses cannot be converted to a loss per unit length, radiation being associated only with discontinuities in the line. In order to estimate the importance of radiation we consider the Q of a half-wave open-end stripline resonator. Radiation from this structure has been calculated by a number of authors, most recently by van der Pauw [22]. Assuming $w \gg s \gg \delta$, van der Pauw's result for the Q due to radiation losses reduces to

$$Q_R = \frac{1}{\mu_o \epsilon_o \omega_o^2 w^2} \frac{\pi^2 \epsilon^{5/2}}{2} \left\{ \frac{(2\epsilon - 1)^2}{3} + \frac{1}{5} \right\}^{-1}, \quad (3.20)$$

where $\omega_o = \pi/\ell \sqrt{\mu_o \epsilon \epsilon_o}$ is the resonant frequency and ℓ is the length of the cavity. The Q due to conduction losses for the same resonator is

$$Q_C = \frac{\mu_o \omega_o s}{2Re[Z_s]}. \quad (3.21)$$

If the characteristic impedance is held fixed (w/s constant) then Q_R increases with miniaturization and Q_C decreases. Davidheiser [23] recently noted this fact and determined the dielectric thickness at which the Q of a superconducting resonator is maximum. Since the ratio Q_R/Q_C decreases with increasing ω_o for both the normal and superconducting cases, there is a resonant frequency above which radiation losses dominate conduction losses. This breakpoint frequency is given in table II for the various striplines considered here assuming $w/s = 10$. For the 0.2 and 2 μm dielectrics, the breakpoint occurs at frequencies higher than those of practical interest and radiation losses can be neglected. For the 20 and 200 μm dielectrics, radiation begins to become important at frequencies around 10^{10} Hz. Since the wavelength is 1.5 cm at 10^{10} Hz for $\epsilon = 4$, microcircuit striplines could be of the right length to approximate a half-wavelength antenna.

While the load at the ends of a microcircuit stripline is not infinite, the radiation from a matched or shorted end is a sizable percentage of that from an open end [24]. Thus radiation losses may well be important at gigahertz frequencies for dielectric thickness greater than 20 μm .

A further consideration omitted from the present calculations regards the propagation of modes of higher order than the assumed TEM mode. Such higher-order modes become possible at frequencies sufficiently high that a half wavelength is comparable to the cross-sectional dimensions of the stripline (10). Assuming $w \gg s$ the cutoff frequency is

$$\omega_c = \pi/w \sqrt{\mu_o \epsilon \epsilon_o}, \quad (3.22)$$

such that for $\epsilon = 4$ and $w = 200 \mu\text{m}$ the cutoff is at 4×10^{11} Hz. Thus, even for striplines of large dimensions in the context of microcircuits, the higher-order modes are important only at frequencies above those of immediate interest.

TABLE II. Frequency (Hz) at which radiation and conduction losses are equal for a half-wave open-ended stripline resonator with $w/s = 10$ and $\epsilon = 4$.

s (μm)	0.2	2	20	200
Cu, 295 K	2.0×10^{13}	1.3×10^{12}	8.0×10^{10}	5.0×10^9
Cu, 4.2 K	1.7×10^{13}	8.9×10^{11}	4.6×10^{10}	2.4×10^9
Nb, 4.2 K	2.6×10^{13}	1.7×10^{12}	1.4×10^9	3.2×10^8

IV. Pulse Propagation

The evaluation of a stripline from the standpoint of pulse transmission follows from a knowledge of γ and Z_o but is sufficiently complicated that simulations prove valuable. In this section we consider the propagation of Gaussian pulses over a stripline of length ℓ using the circuit shown in figure 5. The source/load impedance R_L is matched to the asymptotic high-frequency value of Z_o in the case of a normal-state stripline

$$R_L = \frac{s}{w} \sqrt{\frac{\mu_o}{\epsilon \epsilon_o}}, \quad (4.1)$$

and in the superconducting case is matched to the low-frequency impedance

$$R_L = \frac{s}{w} \sqrt{\frac{\mu_o}{\epsilon \epsilon_o}} \left(1 + \frac{2\lambda}{s} \coth \frac{d}{\lambda} \right)^{1/2}. \quad (4.2)$$

The degree to which a voltage pulse V_S is faithfully reproduced across the load is affected both by γ , in the dispersion and attenuation of the line, and by Z_o , in reflections at the interface between the line and the source or load due to imperfect impedance matching.

The Gaussian pulses considered are of the form

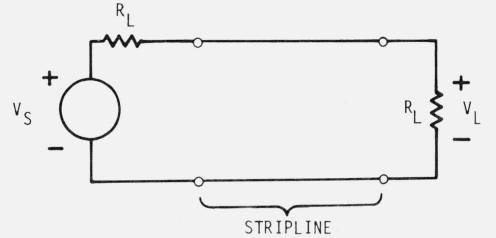


FIGURE 5. Circuit for analysis of pulse transmission.

$$V_S(t) = V_o e^{-t^2/2\tau^2}, \quad (4.3)$$

where the standard deviation τ measures the pulse width. Taking the Fourier transform obtains

$$V_S(\omega) = (2\pi)^{1/2} \tau V_o e^{-\omega^2 \tau^2/2}, \quad (4.4)$$

so that the frequency spectrum is also Gaussian with a standard deviation $\Delta\omega = 1/\tau$. Solving the circuit of figure 5 for the sinusoidal steady-state yields

$$V_L(\omega)/V_S(\omega) = \left(2 \cosh \gamma \ell + \left(\frac{Z_o}{R_L} + \frac{R_L}{Z_o} \right) \sinh \gamma \ell \right)^{-1}, \quad (4.5)$$

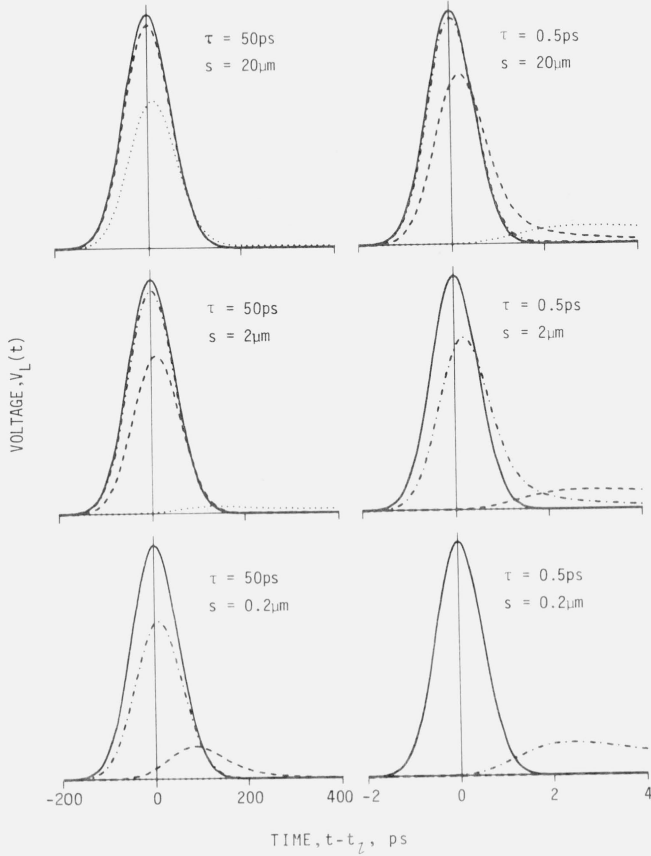


FIGURE 6. Propagation of Gaussian pulses for a copper stripline at 295 K for various dielectric thicknesses, line lengths, and pulse widths.

Pulses are shown for line lengths of zero (solid curve), 0.1 cm (dot-dash), 1 cm (dash), and 10 cm (dot). Curves which essentially coincide with the zero length curve have not been graphed. The time origin is shifted by an amount $t_\ell = \ell/v_\phi(\infty)$ where $v_\phi(\infty) = 1.5 \times 10^8$ m/s is the high-frequency phase velocity.

so that the pulse received at the load takes the form

$$V_L(t) = (2/\pi)^{1/2} \tau V_o \int_0^\infty d\omega e^{-\omega^2 \tau^2 / 2} \times \operatorname{Re} \left[e^{i\omega t} \left(2 \cosh \gamma \ell + \left(\frac{Z_o}{R_L} + \frac{R_L}{Z_o} \right) \sinh \gamma \ell \right)^{-1} \right] \quad (4.6)$$

Numerical evaluation of the above integral was used to determine the shape of a pulse after traversing various lengths of stripline. Since R_L and Z_o are both proportional to $1/w$ these calculations do not depend on the stripline width.

The results of such simulations for copper striplines at 295 K and 4.2 K are shown in figures 6 and 7. For a given dielectric thickness and initial pulse width, pulses are shown as they would appear after traversing striplines of length 0, 0.1, 1, and 10 cm. The time origin for each trace has been shifted by an amount

$$\tau_\ell = \ell/v_\phi(\infty), \quad (4.7)$$

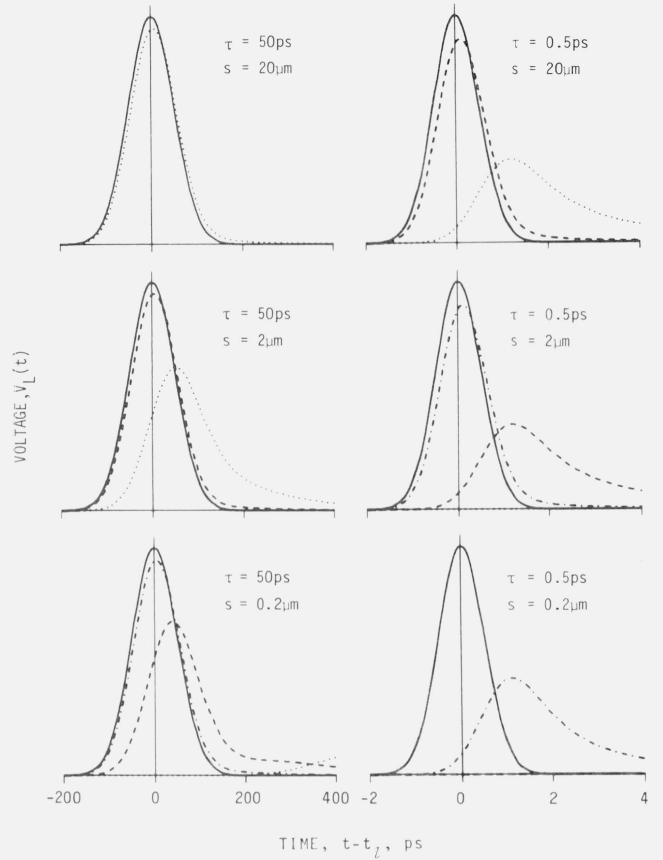


FIGURE 7. Graphs analogous to figure 6 for a copper line at 4.2 K.

such that a pulse traveling at the asymptotic high-frequency phase velocity $v_\phi(\infty)$ would always be centered at the origin. The results shown in the left column of figures 6 and 7 are for a pulse of $\tau = 50$ ps or roughly at the upper limit of speed for present digital circuits. If we arbitrarily require that a pulse be received with at least 80 percent of its original amplitude to be useful in digital applications, then we see from figure 6 that for $s = 20 \mu\text{m}$, $2 \mu\text{m}$, and $0.2 \mu\text{m}$ useful stripline lengths are less than 10 cm, 1 cm, and 0.1 cm, respectively. Thus, the performance of a room-temperature copper stripline with a dielectric thickness of $2 \mu\text{m}$ or less can be a limiting factor even for lengths typical of microcircuit dimensions. At 4.2 K this situation is improved by an order of magnitude in that a dielectric thickness of only about $0.2 \mu\text{m}$ yields lines of sufficient quality for digital microcircuits.

Theoretical arguments indicate that it may be possible to generate pulses with widths as short as 1 ps using superconducting devices [25]. The propagation of such a pulse on normal-state striplines is shown in the right column of figures 6 and 7, using a τ of 0.5 ps to give a full width of about 1 ps. In going from $\tau = 50$ ps to $\tau = 0.5$ ps one notes that the distortion of the shorter pulse is much the same as that of the

longer after propagating only one tenth the distance. Thus, for $\tau = 0.5$ ps, a copper line at 295 K suitable for digital microcircuits requires more than 20 μm of dielectric and at 4.2 K requires more than 2 μm .

Further insight into the transmission of pulses is gained by examining four limiting situations in which the transfer function of eq (4.5) can be simplified. To do this we introduce the series resistance R and inductance L of a unit length of line defined by

$$Z = R + i\omega L \quad (4.8)$$

and the shunt capacitance C per unit length defined by

$$Y = i\omega C \quad (4.9)$$

For the striplines considered here both R and L are in general frequency dependent. The four limits to be discussed result from two different possibilities for Z in combination with two possibilities for the length of the line. If the resistive part of Z is much larger than the reactive part then L can be neglected and we describe the line as being an RC line. The propagation constant and characteristic impedance of the RC line are

$$\gamma = (1 + i)\sqrt{R\omega C/2}, \quad \omega \ll R/L \quad (4.10)$$

$$Z_0 = (1 - i)\sqrt{R/2\omega C},$$

These forms are precisely those which lead to the low-frequency divergences shown in figures 3 and 4 for normal-state lines. Because $Re[Z_s] \ll Im[Z_s]$ for a superconductor, no similar RC behavior occurs in this case. When the reactive part of Z is much larger than the resistive part the line is said to be an LC line and we have

$$\gamma = \frac{R}{2\sqrt{LC}} + i\omega\sqrt{LC} \left[1 + \frac{1}{8} \frac{R^2}{\omega^2 L^2} \right], \quad \omega \gg R/L, \quad (4.11)$$

$$Z_0 = \sqrt{L/C} - i \frac{R}{2\omega\sqrt{LC}},$$

such that γ is nearly pure imaginary and Z_0 is nearly real. The length of a line will be called short or long depending on whether $|\gamma\ell| \ll 1$ or $|\gamma\ell| \gg 1$.

For a short RC line eq (4.5) reduces to

$$V_L/V_S = \frac{R_L}{2R_L + \ell R}, \quad \omega \ll R/L, \quad 1/RC\ell^2, \quad (4.12)$$

where we have assumed $R_L = \sqrt{L/C}$. That is, in the short RC limit the transmission line can be replaced simply by a resistor of value ℓR . The complicated behaviors of γ and Z_0 indicated in eq (4.10) thus combine to give the expected low-frequency result. If the $\Delta\omega$ of a pulse satisfies the conditions of eq (4.12), then the pulse is received with reduced amplitude but unchanged shape. The reduction in amplitude becomes significant if the line is long enough that ℓR is comparable to R_L . For copper at 295 K the length of line for which $\ell R = R_L$ is

$$\ell = \frac{\sigma ds}{2} \sqrt{\frac{\mu_0}{\epsilon\epsilon_0}}, \quad (4.13)$$

so that the useable length increases in proportion to s and d . For $d = 1$ μm and $\epsilon = 4$, this length varies from 0.11 cm at $s = 0.2$ μm to 11 cm at $s = 20$ μm . One concludes that at least 2 μm of dielectric are required to make striplines show sufficiently small amplitude reduction. This is the same conclusion that was drawn from the $\tau = 50$ ps pulses of figure 6 and for good reason. The frequencies below which the various normal-state striplines can be considered RC lines are listed in table III. Since for $\tau = 50$ ps, $\Delta\nu \equiv \Delta\omega/2\pi$ is 3×10^9 Hz, the 295 K lines with $s = 0.2$ μm and 2 μm are on the border between RC and LC lines. Moreover, we shall see that the transfer function of eq (4.12) also applies in the short LC range so that, with the exception of those pulses displaced from the origin, all the 50 ps pulses of figure 6 show the amplitude reduction predicted by eq (4.12).

At 4.2 K one can define a useable length for copper lines at low frequencies similar to that of eq (4.13) but with σ replaced by $\tilde{\sigma}$. This length varies from 7.4 cm at $s = 0.2$ μm to 740 cm at $s = 20$ μm , so that the low-frequency characteristics of cooled copper lines should be very good for lengths typical of microcircuits. As can be seen from table III, however, frequencies considered low are in this case considerably less than those characteristic of a $\tau = 50$ ps pulse.

For a long RC line the frequency response is limited by the RC time constant of the line. The transfer function is

TABLE III. Frequency (Hz) at which the resistive and reactive parts of the series impedance Z are equal for striplines with $d = 1$ μm , $\epsilon = 4$, and various dielectric thicknesses.

s (μm)	0.2	2	20	200
Cu, 295 K	6×10^9	1.5×10^9	2.1×10^8	2.1×10^7
Cu, 4.2 K	7×10^7	2.5×10^7	3.2×10^6	3.2×10^5

$$V_L/V_S = \sqrt{\omega L/R} \exp(-\ell \sqrt{R\omega C/2}) \times \exp\left[-i\left(\frac{\pi}{4} + \ell \sqrt{R\omega C/2}\right)\right], \quad (4.14)$$

$$1/RC\ell^2 \ll \omega \ll R/L,$$

which includes both attenuation and phase lag. Impedance mismatch causes the $\sqrt{\omega L/R}$ attenuation and the $\frac{\pi}{4}$ phase lag. The propagation constant contributes the exponential attenuation and the phase lag proportional to ℓ . The long RC limit describes the 50 ps pulse traveling the $s = 0.2 \mu\text{m}$, $\ell = 1 \text{ cm}$ line shown in figure 6.

In the LC limit, impedance mismatch is present only as a second-order effect and can be neglected. The transfer function in this limit is

$$V_L/V_S = \frac{1}{2} \exp\left(-\ell \frac{R}{2\sqrt{L/C}}\right) \times \exp\left[-i\ell\omega\sqrt{LC}\left(1 + \frac{R^2}{8\omega^2 L^2}\right)\right] \quad (4.15)$$

$$\omega \gg R/L,$$

such that waves propagate with a phase velocity of very nearly $1/\sqrt{LC}$. An LC line is short provided ℓ is much less than the wavelength, $\ell \ll 1/\omega\sqrt{LC}$, and in this case eq (4.15) approximates eq (4.12). Thus, the short RC and LC lines both can be simply modeled with a resistor.

Of the pulses shown in figure 6, all except the 50 ps pulse on the $s = 0.2 \mu\text{m}$ line are described by the transfer function for an LC line, eq (4.15), and the impedance mismatch can be neglected. The propagation of these pulses can be explained in terms of the attenuation and dispersion shown in figure 3. Because Δv is 3×10^9 and $3 \times 10^{11} \text{ Hz}$ for τ equal 50 and 0.5 ps, respectively, the relevant forms for v_ϕ and α_{dB} are approximately those of region III. In this region α_{dB} is proportional to $\sqrt{\omega}$ (see eq (3.12)) so that in going from 3×10^9 to $3 \times 10^{11} \text{ Hz}$ the attenuation increases by a factor of 10. This is confirmed in figure 6 by the fact that the 0.5 ps pulses show the same attenuation as the 50 ps pulses after traveling only $1/10$ the distance. Because α_{dB} is also proportional to $1/s$, an increase in attenuation of a 50 ps pulse on a $2 \mu\text{m}$ line is comparable to that of a 0.5 ps pulse on a $20 \mu\text{m}$ line. A similar conclusion can be drawn for the phase velocity. As eq (3.9) indicates, the deviation of v_ϕ from its high-frequency value is proportional to $1/\sqrt{\omega}s$. The phase shift over a given length of line due to this deviation is thus proportional to $\sqrt{\omega}/s$. Thus, broadening of a pulse and displacement of its peak from $t = t_\ell$ change with ω and s just as the attenuation.

The LC approximation applies to all of the pulses shown in figure 7 for copper at 4.2 K. For frequencies typical of the

pulses shown the surface impedance is governed by the extreme-anomalous equations with $\delta_a < s, d$. In this limit, the attenuation and phase shift are proportional to $\omega^{2/3}/s$. Conclusions similar to those drawn for copper at 295 K can thus be made for figure 7.

An analysis of pulse propagation for superconducting niobium is shown in figure 8 for pulses with $\tau = 1$ and 0.5 ps. For a pulse with $\tau = 50 \text{ ps}$ there is no significant distortion even after propagating a distance of 10 cm on a line with $0.2 \mu\text{m}$ of dielectric. Pulse degradation is essentially negligible for superconducting lines until the frequencies involved begin to approach the energy-gap frequency, at which point the stripline characteristics degrade rapidly. The increase in distortion between the 1 and 0.5 ps pulses of figure 8 is thus nearly as great as that between 50 and 0.5 ps pulses on a normal-state stripline. The distortion evident in figure 8 is primarily due to dispersion at frequencies somewhat below the energy gap as discussed elsewhere in detail [13]. Comparison of figures 7 and 8 shows that a superconducting line is marginally superior to a normal-state line even for $\tau = 0.5 \text{ ps}$. For longer pulses the superiority of superconducting lines is beyond question.

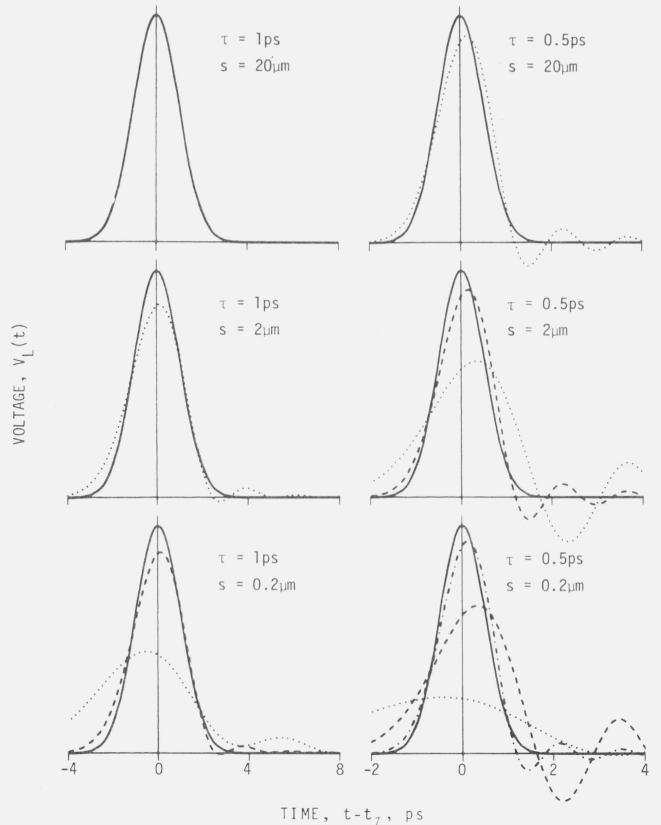


FIGURE 8. Graphs analogous to figure 6 for a niobium line at 4.2 K. The time origin is shifted by an amount $t_\ell = \ell/v_\phi(0)$ where the low-frequency phase velocity $v_\phi(0)$ is 1.10×10^8 , 1.44×10^8 , and $1.49 \times 10^8 \text{ m/s}$ for dielectric thickness of 0.2, 2, and $20 \mu\text{m}$, respectively.

V. Appendix

The numerical solution of eq (2.7) and calculation of the surface impedance for general l , δ_c , and d follows a method presented by Mason and Gould [26] for the superconducting case. Applying the transformations of Mason and Gould to eq (2.7) yields

$$E_x(z) = E_x(d) + i \frac{\alpha}{l} \int_0^d dz' E_x(z') \cdot G_1((z' - d)/l, (z' - z)/l) \quad (\text{A.1})$$

$$G_1(u, v) = \int_u^v dr \int_1^\infty ds (v - r) \left(\frac{1}{s} - \frac{1}{s^3} \right) e^{-|r|s},$$

where the kernel G_1 can be evaluated in terms of E_1 , the exponential integral [27]. Over the domain of interest ($u \leq 0, v \geq u$),

$$\begin{aligned} G_1(u, v) &= \frac{1}{24} [(u^3 + u^2 - 10u - 6)e^u \\ &\quad + (u^4 - 12u^2)E_1(|u|)] \\ &\quad + \frac{1}{24} [(|v^3| - v^2 - 10|v| + 6)e^{-|v|} \\ &\quad + (v^4 - 12v^2)E_1(|v|)] \quad (\text{A.2}) \\ &\quad + \frac{1}{6} (v - u)[(u^2 + u - 4)e^u \\ &\quad + (u^3 - 6u)E_1(|u|)] \\ &\quad + \frac{2}{3} (|v| + v) \end{aligned}$$

A numerical solution of the above integral equation results when the integral is approximated by a sum consisting of N terms in which the integrand is evaluated at the points $z' = z_1, z_2, \dots, z_N$. By choosing z to be each of these z_i in succession, one obtains a set of N linear equations which can be solved for the unknowns $E_x(z_i)$. In this procedure $E_x(d)$ may be taken as any non-zero constant as it merely sets the scale.

Once $E_x(z)$ is known, the integral over current density required for the surface impedance can be obtained from

$$\begin{aligned} \int_0^d dz J_x(z) &= \frac{3}{4} \sigma \int_0^d dz E_x(z) G_2((z - d)/l, z/l) \\ G_2(u, v) &= \int_u^v dr \int_1^\infty ds \left(\frac{1}{s} - \frac{1}{s^3} \right) e^{-|r|s}, \end{aligned} \quad (\text{A.3})$$

where for the domain of interest ($u \leq 0, v \geq 0$),

$$\begin{aligned} G_2(u, v) &= \frac{4}{3} + \frac{1}{6} [(u^2 + u - 4)e^u + (u^3 - 6u)E_1(|u|)] \\ &\quad + \frac{1}{6} [v^2 - v - 4)e^{-v} - (v^3 - 6v)E_1(v)]. \quad (\text{A.4}) \end{aligned}$$

The above procedure gives accurate results using a small number of integration points except when the depth of field penetration is small compared to d . In this limit, however, d can be taken as infinity and the Reuter-Sondheimer result, eq (2.8), adopted in place of the integral equation.

VI. References

- [1] Van Tuyl, R. L., Liechti, C. A., Lee, R. E., and Gowen, E. GaAs MESFET Logic with 4-GHz Clock Rate, IEEE J. Solid-State Circuits, Vol. **SC-12**, pp. 485-496, (Oct. 1977).
- [2] Herrell, D. J. Femtojoule Josephson Tunneling Logic Gates, IEEE J. Solid-State Circuits, vol. **SC-9**, pp. 277-282, (Oct. 1974).
- [3] Keyes, R. W. Physical Limits in Digital Electronics, Proc. IEEE, vol. **63**, pp. 740-767, (May 1975).
- [4] Keyes, R. W., Harris, E. P., Konnerth, K. L. The Role of Low Temperatures in the Operation of Logic Circuitry, Proc. IEEE, vol. **58**, pp. 1914-1932, (Dec. 1970).
- [5] Hasan, M. M. and Mullick, S. K. Monolithic MIC's, in *Microwave Integrated Circuits*, K. C. Gupta and A. Singh, Eds. (New York: Wiley, 1974).
- [6] Lahiri, S. K. and Basavaiah, S. Lead-Alloy Josephson-Tunneling Gates with Improved Stability upon Thermal Cycling, J. Appl. Phys., vol. **49**, pp. 2880-2884, (May 1978).
- [7] Bryant, T. G. and Weiss, J. A. Parameters of Microstrip Transmission Lines and Coupled Pairs of Microstrip Lines, IEEE Trans. Microwave Theory Tech., vol. **MTT-16**, pp. 1021-1027, (Dec. 1968).
- [8] Herrell, D. J., Arnett, P. C. and Klein, M. High Performance Josephson Interferometer Latching Logic and Power Supplies, in *Future Trends in Superconductive Electronics*, B. S. Deaver et al. Eds. (New York: American Institute of Physics, 1978), pp. 470-478.
- [9] Denlinger, E. J. A Frequency Dependent Solution for Microstrip Transmission Lines, IEEE Trans. on Microwave Theory Tech., vol. **MTT-19**, pp. 30-39, (Jan. 1971).
- [10] Corr, D. G. and Davies, J. B. Computer Analysis of the Fundamental and Higher Order Modes in Single and Coupled Microstrip, IEEE Trans. on Microwave Theory Tech., vol. **MTT-20**, pp. 669-678, (Oct. 1972).
- [11] Matick, R. E. *Transmission Lines for Digital and Communication Networks*. (New York: McGraw-Hill, 1969), Chapters 4 and 6.
- [12] Mattis, D. C. and Bardeen, J. Theory of the Anomalous Skin Effect in Normal and Superconducting Metals, Phys. Rev., vol. **111**, pp. 412-417, (July 1958).
- [13] Kautz, R. L. Picosecond Pulses on Superconducting Striplines, J. Appl. Phys., vol. **49**, pp. 308-314, (Jan 1978).
- [14] Tinkham, M. *Introduction to Superconductivity*. (New York: McGraw-Hill, 1975), Chapters 2 and 3.
- [15] Pippard, A. B. Metallic Conduction at High Frequencies and Low Temperatures, in *Advances in Electronics and Electron Physics*, vol. **VI**, L. Marton, Ed. (New York: Academic Press, 1954), pp. 1-45.
- [16] Reuter, G. E. H. and Sondheimer, E. H. The Theory of the Anomalous Skin Effect in Metals, Proc. Roy. Soc., (London), vol. **A195**, pp. 336-364, (Dec. 1948).

- [17] *American Institute of Physics Handbook*, D. E. Gray, Ed. (New York: McGraw-Hill, 1972), p. 9-39.
- [18] Rosenblum, S. S., Steyert, W. A., and Fickett, F. R. A Simple Method for Producing High Conductivity Copper for Low Temperature Applications, *Cryogenics*, vol. **17**, pp. 645-647, (Nov. 1977).
- [19] Henkels, W. H. and Kircher, C. J. Penetration Depth Measurements on Type II Superconducting Films, *IEEE Transactions on Magnetics*, vol. **MAG-13**, pp. 63-66, (Jan. 1977).
- [20] Sondheimer, E. H. The Mean Free Path of Electrons in Metals, *Advances in Phys.*, vol. **1**, pp. 1-42, (Jan 1952).
- [21] Ramo, S., Whinnery, J. R., and Van Duzer, T. *Fields and Waves in Communication Electronics*. (New York: Wiley, 1965), p. 334.
- [22] van der Pauw, L. J. The Radiation of Electromagnetic Power by Microstrip Configurations, *IEEE Trans. Microwave Theory Tech.*, vol. **MTT-25**, pp. 719-725, (Sept. 1977).
- [23] Davidheizer, R. A. Superconducting Microstrip Filters, in *Future Trends in Superconductive Electronics*, B. S. Deaver et al. Eds., (New York: American Institute of Physics, 1978), pp. 219-222.
- [24] Lewin, L. Radiation from Discontinuities in Strip-Line, *Proc. IEE*, vol. **107C**, pp. 163-170, Feb. 1960.
- [25] McDonald, D. G., Peterson, R. L. and Bender, B. K. Design of a Josephson-Junction Picosecond Pulser, *J. Appl. Phys.*, vol. **48**, pp 5366-5369, (Dec. 1977).
- [26] Mason, P. V. and Gould, R. W. Slow-Wave Structures Utilizing Superconducting Thin-Film Transmissions Lines, *J. Appl. Phys.*, vol. **40**, pp. 2039-2051, (April 1969).
- [27] *Handbook of Mathematical Functions*, M. Abramowitz and I. A. Segun, Eds. (New York: Dover, 1965), p. 228.